Eleventh International Conference on the Bearing Capacity of Roads, Railways and Airfields, Volume 3 – Hoff, Mork & Saba (eds)

Investigation of local rail track deterioration due to sleeper support condition variation

N. Lillin, D. Rudisch & S. Freudenstein
Chair and Institute of Road, Railway and Airfield Construction, Technical University of Munich, Munich, Germany

F. Mitlmeier, F. Kotter & C. Moormann
Institute of Geotechnical Engineering, University of Stuttgart, Stuttgart, Germany

ABSTRACT: Varying sleeper support (e.g. seat stiffness) influences the load distribution of the track. Consequently, this might result in locally accelerated ballast and substructure deterioration, including mud spot development.

A vehicle-track-subgrade modelling workflow has been developed to investigate the interaction between its elements. The comprehensive approach incorporates track irregularities, vehicle dynamics, varying sleeper support and complex ballast and soil modeling, including ballast contamination.

Measurements have been conducted at two track sections with known subgrade problems, including a former and possibly reoccurring mud spot. Based on these measurements, calibration and validation parameters for the models are derived, as a case study. Individual rail seat stiffness values could be identified with an iterative approach, using strain and deflection measurement data and a finite element model.

The presented study demonstrates that the identified high variation in rail seat stiffness at the former mud spot leads to individual sleepers with significantly increased load transmission to the ballast. It also highlights the limitation of the loaded geometry, as measured by track recording cars, to reflect the rail seat stiffness variation.

Keywords: Vehicle-track-subgrade interaction, trackside measurements, rail support stiffness variation, mud spot

1 INTRODUCTION

Immaculately built and maintained ballasted rail tracks distribute the vehicle loads evenly across the track through the ballast to the substructure. In practice, railroad tracks can have imperfections like varying support conditions of the sleepers in the ballast bed.

Varying sleeper support (e.g. seat stiffness) influences the local rail deflections and can result in significant local increases of the forces transmitted from particular sleepers to the ballast. Consequently, the locally increased dynamic interactions can lead to locally accelerated ballast and substructure deterioration.

Locally increased dynamic forces and cohesive and saturated soils (e.g. due to lack of drainage performance) may induce mud spots (Rapp, 2017). A mud spot can lead to a rapid track deterioration, including the development of track geometry faults, which supersede safety thresholds and compromise safe train passages (Hudson et al., 2016).

DOI: 10.1201/9781003222910-21

A comprehensive numerical simulation workflow has been established to analyze the interaction between vehicle, track and subgrade during train passages over tracks with support layer problems. Those include varying rail seat support and ballast contamination, which can occur at mud spots.

A measurement site with known subgrade problems has been selected as a case study, at a former mud spot and a reference site. Different measurements have been conducted to provide realistic input values for the developed methodology and to evaluate the results.

The presented study focuses on the investigation of the effects of varying rail seat stiffness.

2 MEASUREMENTS & SUPPORT STIFFNESS IDENTIFICATION

2.1 *Measurement site*

To investigate the track behavior in a case study at a single-track railway line with known subgrade problems, an in-service track section has been selected where mud spots have developed in the past. Track geometry measurements have been carried out and geotechnical information has been gathered. Two 14.5m sections in close proximity have been selected to carry out track deformation measurements during train passages.

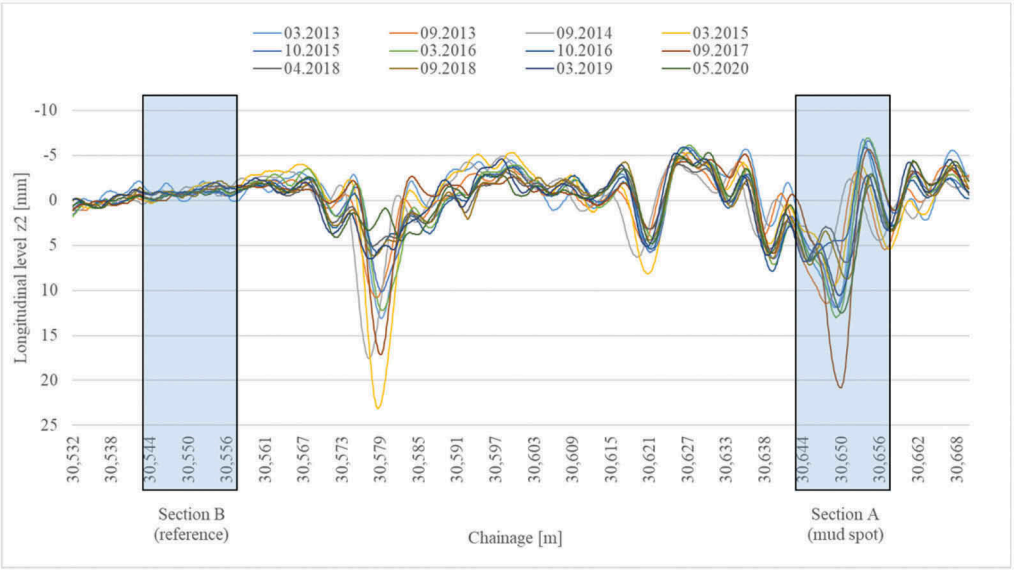

Figure 1. Loaded vertical geometry of right rail – RAILab measurements 2013-2020 – selected measurement sites.

Section A represents a former mud spot, which has been maintained locally two years prior to the track deformation measurements of the presented study. The development of the mud spot can be observed in the analysis of the loaded geometry, represented by track measurement data by a RAILab measurement train by Deutsche Bahn (see Figure 1). The maintenance measure included replacing ballast, sleepers and fastening systems and introducing a geotextile layer between subgrade and the replaced ballast. Two years after maintenance, fine particles can be observed in the ballast (see Figure 2), indicating the reappearance of a mud spot.

Figure 2. Ballast cross section at (former) mud spot – Measurement section A.

Section B is at a distance of 100m to the first section. It has the same track characteristics and geotechnical boundary conditions, but did not show any progression in the analysis of the loaded geometry (see Figure 1). Hence, section B was selected as a reference section.

2.2 *Unloaded and loaded track geometry*

Track recording cars measure the track geometry under their vehicle load usually under the permissible track operating speed (DB Netz AG, 2016). This *loaded track geometry* is supposed to represent the safety critical track defects. On the other hand, the *unloaded track geometry*, recorded by hand-driven measurement carts, represents the track geometry without the influence of vehicle mass and vehicle speed.

The vertical loaded track geometry, recorded by RAILab measurement vehicles, were used to analyze the track section and for selection of the measurement site (see chapter 2.1).

The unloaded track geometry was measured on a 1000m section with an inertial measurement unit AMU 1030, mounted on a hand driven measurement cart GRP 3000 IMS, both by the company Amberg Technologies. For the purpose of the presented study, only the vertical geometry of the two rails was considered. To reduce the influence of the track layout (here: longitudinal inclination changes) a band pass filter has been applied to the dataset. The used Butterworth filter has a low cutoff wavelength of 3m and a high cutoff wavelength of 70m, comparable to the filter characteristics used by RAILab data filter (Sandner et al., 2020). The measured vertical track geometry of both rails was used to calculate rail-wheel forces (see chapter 3.1). Due to the measurement system and the filter characteristics short-wavelength track defects are not included in the determination of rail-wheel forces.

By processing both loaded and unloaded vertical track geometry equivalently, and eliminating the influence of the track layout, the resulting difference between both signals can be attributed to the load-dependent deflection of the rails under the dynamic load of the measurement vehicle. This difference might vary along the track due to variations in track stiffness.

Figure 3 shows a fictitious example, where for illustration purposes the absolute track geometry is displayed by introducing a difference between loaded and unloaded vertical track geometry, representing the rail deflection under load. The blue line describes the unloaded vertical track geometry, while the green line, assuming a constant deflection under the vehicle load of 1.5mm, represents the loaded track geometry. The red line illustrates a section with reduced stiffness, as one might expect at a developed mud spot. In this imaginary example, the reduced stiffness at the mud spot causes a deviation of the loaded from the unloaded vertical

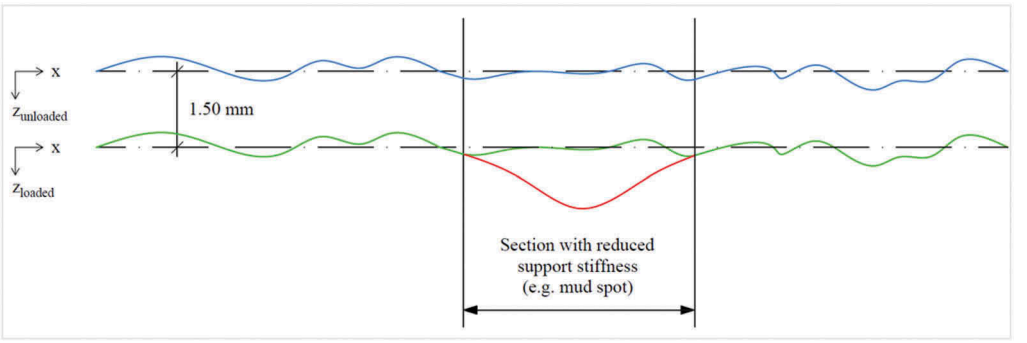

Figure 3. Concept of unloaded (blue line) and loaded (green line) vertical geometry – example of locally reduced stiffness, as would be expected at mud spot (red line).

track geometry. The resulting loaded track geometry signal contains both the influence of the unloaded geometry and the varying stiffness. With appropriate signal processing, possibly under the additional use of unloaded track geometry measurements, the stiffness variation can be identified.

2.3 *Track deformation measurements*

To provide input for the numerical models as a case study and to validate the results, high frequency track deformation measurements have been carried out representatively on the right rail at the two mentioned 14.5m sections, with identical instrumentation. All sensors of both sites were collected at one computer to obtain simultaneous results with a common time signal.

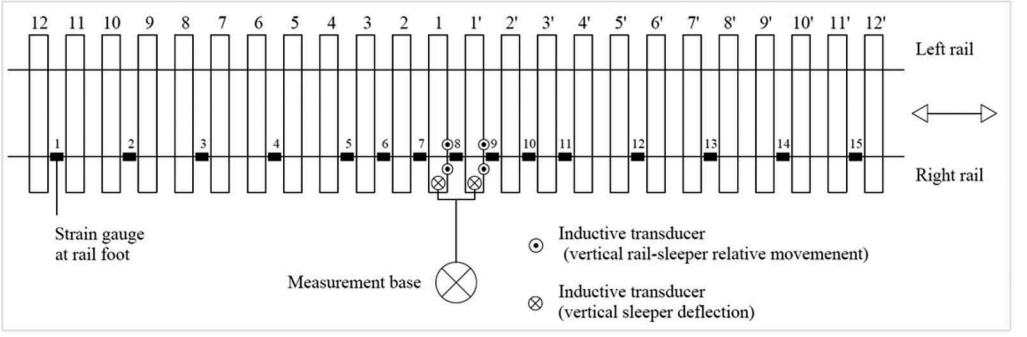

Figure 4. Identical instrumentation of both measurement sites.

Per measurement site, fifteen strain gauges have been attached each to the rail foot in the center of the sleeper compartment to measure the rail foot strain and to obtain information about the bending moment of the rail during train passage. In the center of each section, strain gauges were fitted in every sleeper compartment. Towards the edges of each section, every second compartment has been equipped with a sensor, to obtain information about the bending behavior of a longer section (see Figure 4).

Inductive transducers connected to the two centered sleepers of each sections recorded the vertical deflection of the sleepers during train passage. The inductive transducers have been attached to a measurement base mounted on a drainage shaft, to reduce the influence of soil vibration. Additionally two inductive transducers per sleeper measured the relative vertical movement between rail and sleeper (see Figure 4).

Multiple train runs, of both passenger trains and freight trains, have been recorded and analyzed. The train run of two BR218 locomotives, without additional wagons, was selected for the purpose of the present study.

2.4 *Identification of rail seat stiffness*

As uneven sleeper support might have an important impact on vehicle-track-subgrade interaction (Dahlberg, 2010) it is also incorporated in the proposed coupled workflow (see chapter 4) and thus had to be identified at the measurement site.

Although varying sleeper support might have various reasons, like changing subgrade properties, crushed or contaminated ballast or voided sleepers, they result in uneven rail deflection under a specific load along a track (see chapter 2.2). Measuring only rail deflections under a specific load along a track, e.g. with Benkelman measurements (Leykauf et al., 1997) does not allow the determination of sleeper-specific stiffnesses. Since the deflection of a specific point along the rail is not only influenced by the sleeper below this section of rail, but also by neighboring sleepers, due to the bending stiffness of the rail.

To identify sleeper-specific seat stiffnesses a procedure using measurement data and a finite element model has been developed, inspired by (Chen et al. 2018). In this procedure specific load positions of the measurements are replicated in the finite element model created in ANSYS, simplifying seat stiffness as linear-elastic support of the rail. The 20m long 2D finite element model represents the bending stiffness of the measured right rail as a beam and the vertical stiffness of the rail support by discrete supports, assumed as linear-elastic, in the distance of sleeper spacing. Individual load positions of the measurement have been reproduced in the model by placing single loads on the rail, primarily the first axle of the locomotive BR218 on each sleeper compartment. By iteratively adjusting the seat stiffnesses at each load position, a combination of seat stiffness values could be identified, so that the rail foot strain in the model corresponds to the strain under the equivalent rail foot position in the measurement. Subsequently, load cases with the first two axles of the BR 218 locomotives have been tested on the model (see Figure 5) and showed only minor deviations. The same procedure with different train runs each resulted in similar stiffness ratios, therefore the identified stiffness ratio is realistic and can be used for purposes of the here presented case study. Additionally, the measured sleeper deflections at the two sleepers have been used to calibrate the final rail seat stiffness values, since the initial valued did not result in the correct rail deflection as measured. This is necessary, because some input values of the seat stiffness identification process might not have been accurate. Input values with possible errors include the unknown dynamic wheel forces, the actual value of the bending stiffness of the rail or the fact, that the effective distance between two sleepers is not equal to the distance of the sleeper centers.

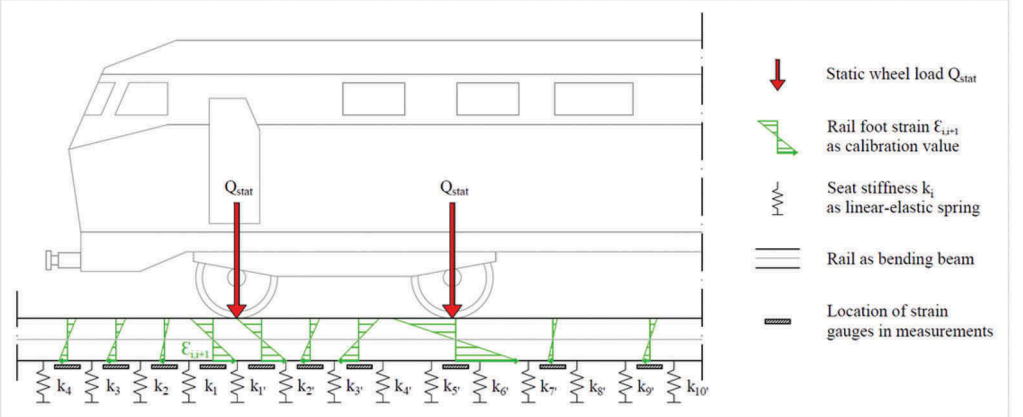

Figure 5. Model to identify rail seat stiffness variation (locomotive for illustration purposes).

Hence, the identified and for the case study selected seat stiffnesses result in sleeper deflections, which are in agreement with the measurements. Additionally, the ratio of stiffnesses per section results in rail foot strain values, which are in agreement with the ratio of stiffnesses in the measurements (see Figure 6).

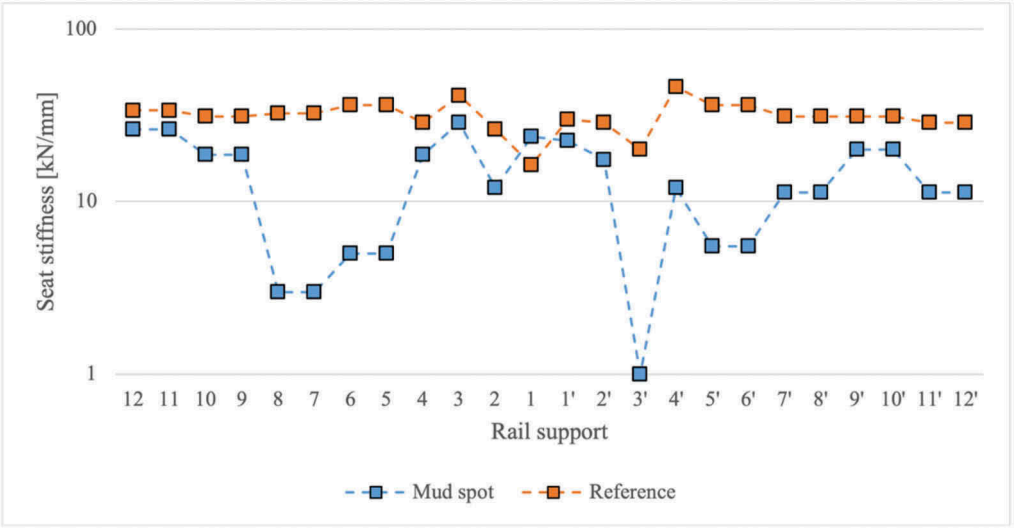

Figure 6. Identified rail seat stiffnesses at the two measurement sections.

One can observe that section A, the former mud spot, has a high variation of stiffness, and section B has a significantly lower variation. Even if the exact values might differ somewhat, and are influenced by nonlinearities, like voided sleepers, the variation from sleeper to sleeper is still large. Variations up to factor 17.5 can be observed from one sleeper to the next, approximating the rail support as linear-elastic. It is noteworthy, that the identified seat stiffnesses at the former mud spot (measurement section A), although displaying high variation, show no reduction in stiffness towards a conceivable center of the mud spot, as it could have been expected (see Figure 3).

This leads to the conclusion that varying rail seat stiffness has to be included in the analysis of the vehicle-track-subgrade interaction of this track. The resulting stiffnesses were used as a close-to-reality example in the presented case study for the coupled vehicle-track-subgrade interaction model (chapter 3.1).

3 SIMULATIONS

3.1 *Coupled vehicle-track-subgrade interaction modelling*

The goal of the presented methodology for coupled vehicle-track-subgrade interaction modeling is to create a tool to investigate the interaction between vehicle, track and subgrade comprehensively in an integral approach. It combines the effects of 3D vehicle-track interaction, the vertical load distribution of a flexible track with varying support stiffness and the ballast and subgrade reaction with complex soil models and soil properties. Thereby, the influence of each parameter and the resulting interdependencies can be analyzed. In the presented study, the focus lies on the influence of varying support conditions. Firstly the resulting impact on the ballast and possible deterioration of the track components and secondly the resulting vehicle reaction, and possible vehicle-side detectability of support stiffness variations.

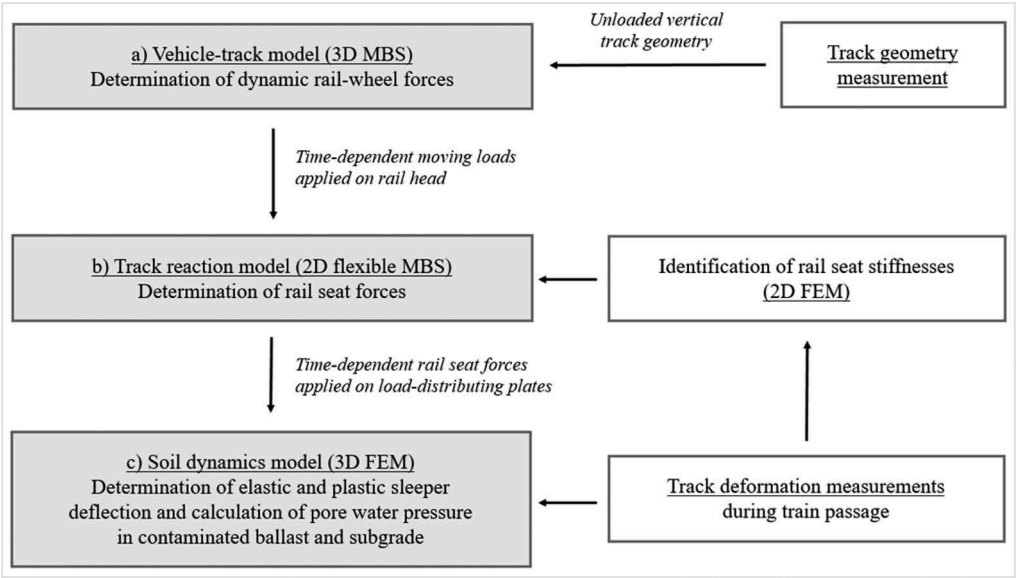

Figure 7. Workflow of the presented methodology.

Figure 7 shows the elements of the methodology and the workflow and dataflow between the steps of the procedure. Figure 8 illustrates the modelling steps.

Model step a) is a 3D multi body simulation model, created in the software SIMPACK. It comprises a bogie model, in this case representing a bogie of the BR218 locomotive, running on a 500m long three-dimensional track, with the measured unloaded track geometry as track-side excitations. It comprises a complex rail-wheel contact model, taking into account the rail-head and wheel profile. The running behavior of the bogie, or alternatively a whole railway vehicle, can be investigated in this model, but is not the focus of this study. The main purpose of *model step a)* is the calculation of rail-wheel-forces, due to the interaction between vehicle and track, with the measured geometry. A vehicle velocity of 30m/s was chosen for the simulation corresponding to the velocity of the locomotives during the measurement run (ca. 32m/s).

Exemplarily Figure 9 shows the calculated rail-wheel-forces for the first wheelset of the locomotive BR 218.

Model step b) is a flexible 2D multi body simulation model created in the software SIMPACK. It represents the bending and load distributing behavior of one rail on discrete support points. A flexible Timoshenko beam represents the stiffness of the rail. The support points are modeled as linear-elastic springs. The stiffness values of the rail seat stiffnesses determined in chapter 2.4 were assigned to the springs in the center of the 86 m long model. Moving time-dependent loads are applied on the rail to represent the train run of the two BR 218 locomotives. Separately the rail-wheel forces of the right and the left wheels of *model step a)* are used, with the same progress speed (30m/s) as in that model. *Model step b)* is able to calculate the deflection and the rail seat forces of the rail under the moving loads. The latter represent the loads transmitted through half sleepers in the ballast. Consequently the partial sleeper mass is added to the rail seat forces.

Figure 10 shows an exemplary section of rail seat forces of seven consecutive sleepers subjected to the passage of one bogie of the locomotive BR 218. In this example sleeper 3, sleeper 4 and sleeper 9 are surrounding less supported sleepers 5 to 8. Thus a large part of the load is transferred trough the well supported sleepers, represented by high (positive) compression forces. The linear-elastic assumption of the support points causes an overestimation of the (negative) tensional forces. The tensional rail seat forces do not affect the subsequent simulations, as tension forces are not applied on the 3D continuum model of *model step c)*.

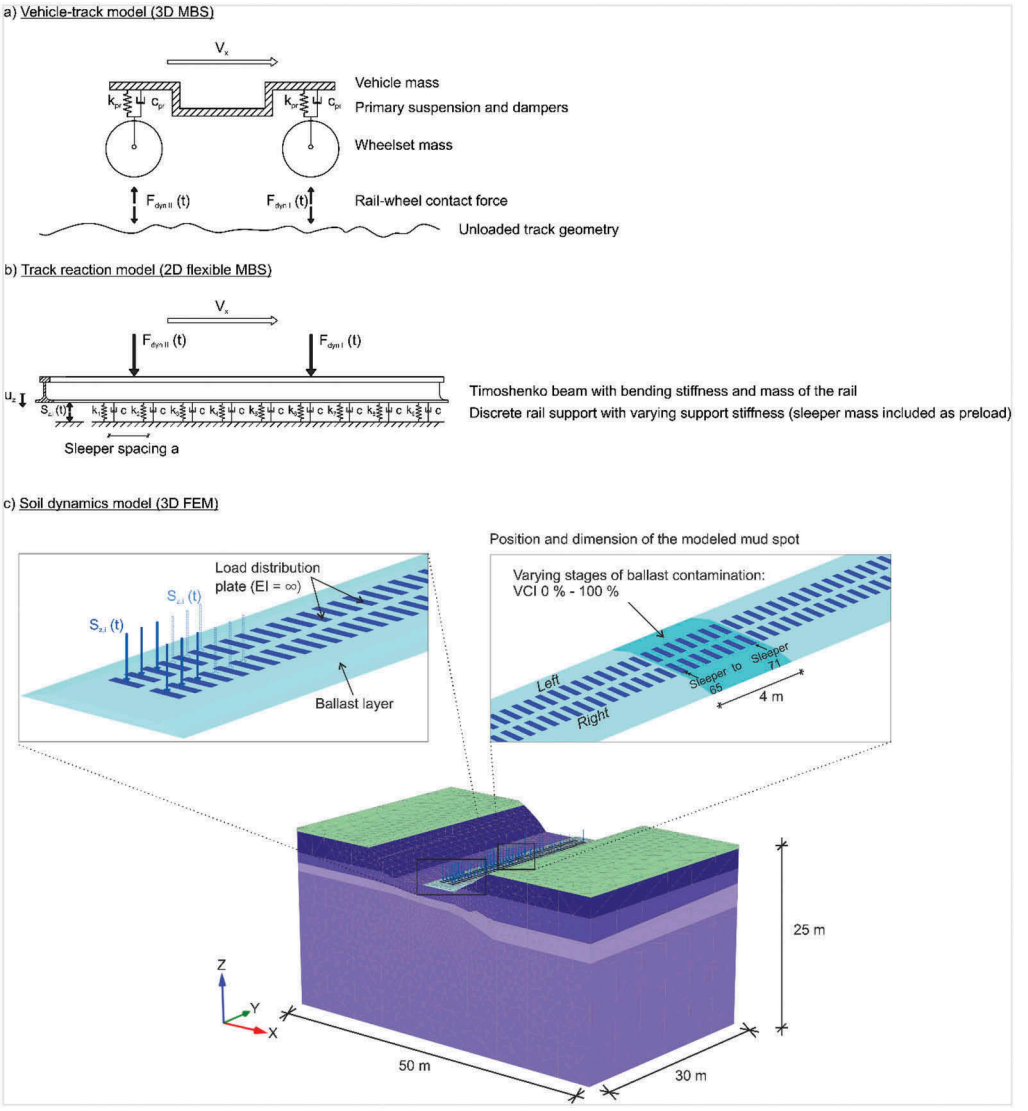

Figure 8. Illustrations of the simulation steps of the workflow.

Model step c) is a 3D finite element model, created in the software PLAXIS. The dynamic 3D continuum model represents the ballast body and the surrounding soil and embankment. A hypoplastic soil model is used to calculate plausible elastic and plastic deformations as well as pore water pressure throughout the continuum. The properties of the model have been calibrated by provided geotechnical exploration data from the measurement section. Stiff load plates, representing each a half sleeper sole minus a support-free center section, apply the time-dependent rail seat forces calculated in *model step b)*. The resulting elastic deflections under the sleeper sole have been validated by the sleeper deflection measurements (see chapter 2.3).

As an example for the generated output, Figure 11 shows plastic deformations under the sleepers for various ballast contamination levels, representing the accumulation of fine particles in the ballast body after track operation. The used Void Contaminant Index (VCI) was proposed in (Tennakoon, 2012) and corresponds to different levels of ballast contamination, which can be expected during mud spot development.

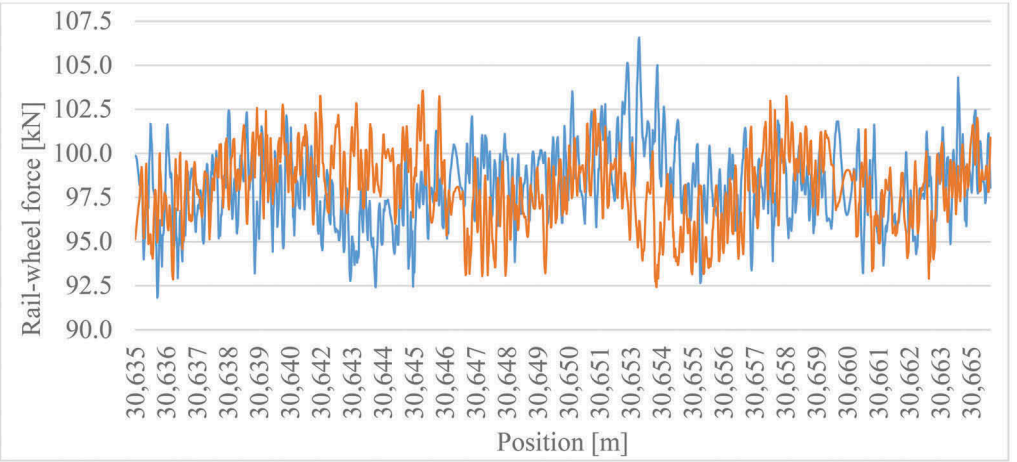

Figure 9. Sample of rail-wheel-forces calculated by *model step a)* – front left wheel (orange line); front right wheel (blue line).

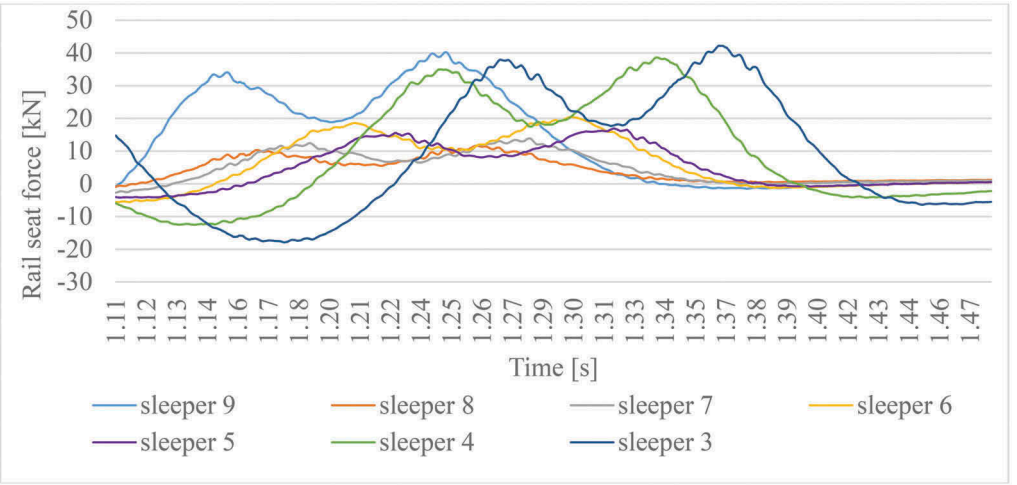

Figure 10. Sample of sleeper support forces calculated by *model step b)*.

3.2 *Results and discussion*

Figure 12 contains results of *model step b)* for both sections of the case study. It shows the vertical rail deflection and the corresponding rail seat forces, in case the first wheel of the locomotive BR 218 is at the respective sleeper position.

At section A, representing the former mud spot, a large variation in rail seat force can be observed. From one sleeper to the next one variations up to factor eight occur. This is less than the determined variation of rail seat stiffness at this track section (see chapter 2.4) but still significant. The variation leads to the fact that individual sleepers transmit significantly more load to the ballast, than others do. Figure 10 also illustrates the highly changed load distribution of the track. It can be expected that ballast deterioration increases locally under the sleepers with high load transmission, during thousands of axle transitions in the course of train operations on the investigated track. Possibly, there is also a locally increased impact on the soil.

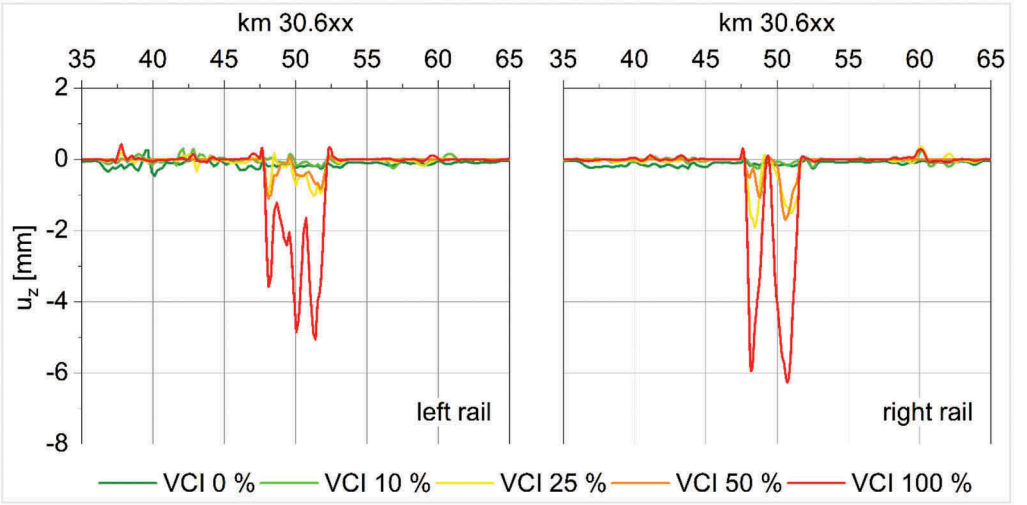

Figure 11. Sample of plastic deformations u_z under the sleepers calculated by *model step c)*.

At section B, representing the reference site, the maximum rail seat forces are much more homogeneous and only small variations are observed.

Figure 13 illustrates that the variation in rail seat force can be attributed primarily to the rail seat stiffness variation. Although it is not possible to draw a clear causal line from the stiffness variation at the former mud spot to mud spot development in general, it is noticeable, that the identified seat stiffness varies much more at the mud spot section, than at the reference section (see also Figure 12). In addition, the reference section did not show any signs of major changes in track geometry in the past, unlike the former mud spot (see Figure 1). Moreover, two years after the maintenance the accumulation of fine particles in the ballast indicates that the mud spot may be reappearing (see Figure 2).

In conclusion, a correlation between the reappearing mud spot and the observed rail seat stiffness variation is present. Together with the presented results that sleeper support variation leads to a changed load distribution of the track and to individual sleepers with high load transmissions, the significance of rail seat stiffness variation to the deterioration of the track becomes evident.

Further investigation needs to be done, to determine the causal relationships during mud spot development and other track deterioration phenomena. The present study highlights that seat stiffness variation should be considered.

3.1.1 *Identification of seat stiffness variation in track inspection*

As demonstrated, sleeper support condition variation leads to changed load distribution, higher local deterioration and subsequently to possible track defects. The necessity for a well-maintained and consequently homogeneous track structure is obvious. However, as most tracks are subject of continuous train operations and maintenance resources are limited, the need arises to identify sections with varying support stiffness during track inspection, to facilitate timely and effective measures.

Track inspection uses mainly loaded geometry measurements (e.g. RAILab). The vertical loaded geometry signals can contain some information about the stiffness along the track, as illustrated in Figure 3. With suitable signal processing, this information can possibly be extracted and used.

On the other hand Figure 12 shows, that seat stiffness variation between individual sleepers do not always manifest in the rail deflections under the wheel load (e.g. sleeper number 4′), especially evaluated only at the sleeper positions. Hereby, the evaluation of rail deflections under a wheel load corresponds to the stiffness component of the loaded track geometry. Even if it is evaluated continuously (see Figure 13) individual rail seat stiffnesses hardly

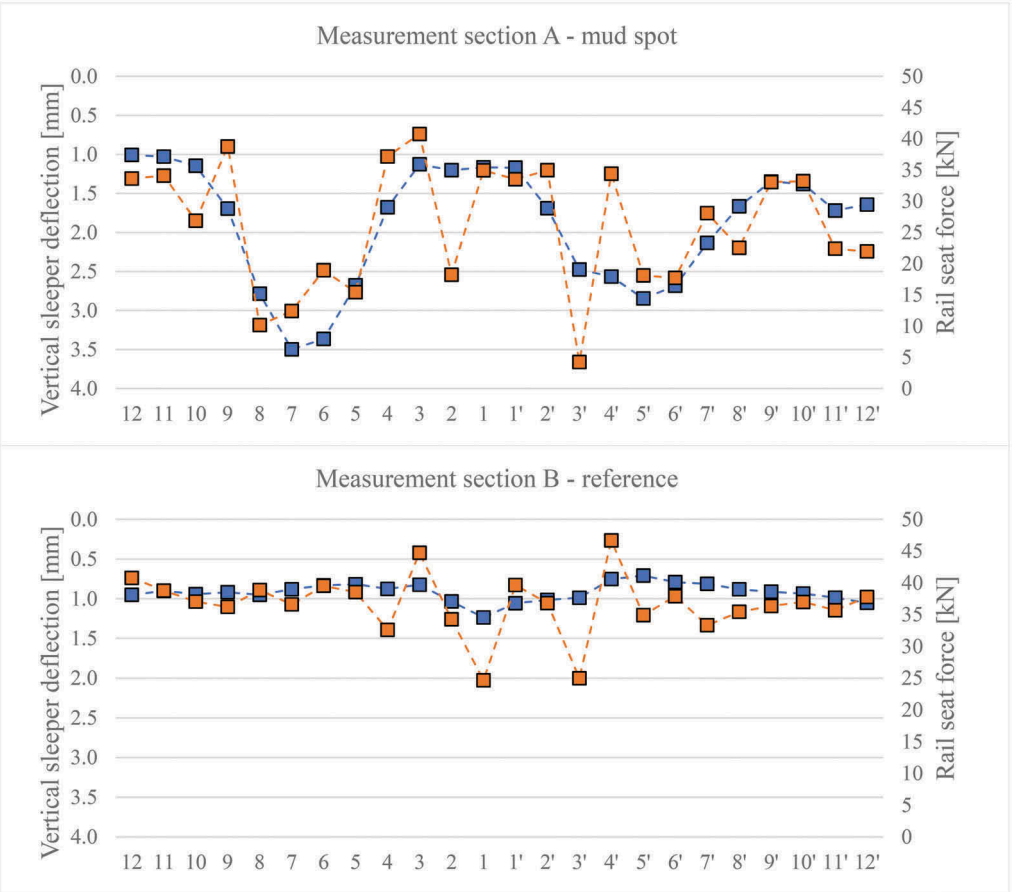

Figure 12. Rail deflection in case the first wheel of the locomotive is over a specific sleeper (blue markers) and corresponding rail seat forces (orange markers).

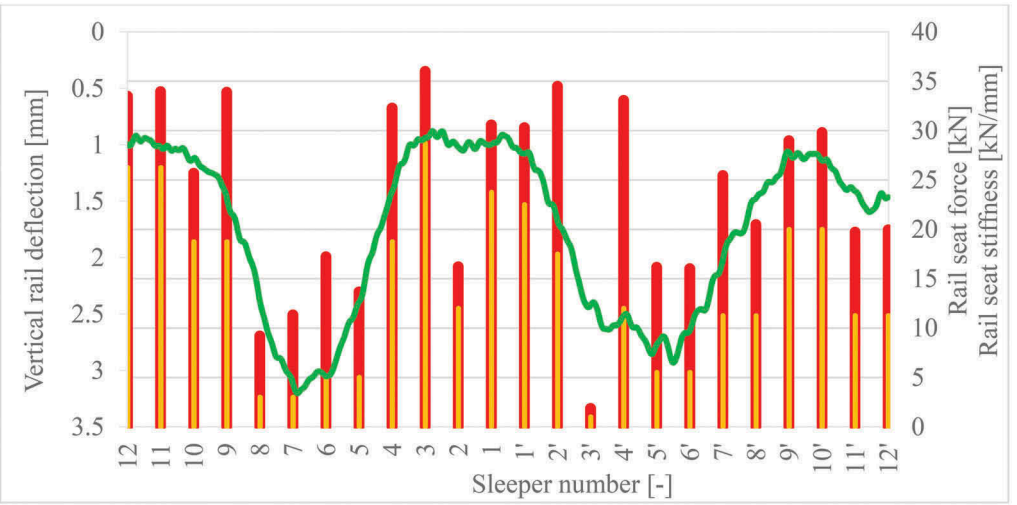

Figure 13. Results along measurement site A "mud spot": Rail deflection under the first wheel of the locomotive (green line); rail seat force of specific sleeper in case the first wheel of the locomotive is over that rail seat (red bars); rail seat stiffness for corresponding sleeper (orange bars).

manifest in the loaded track geometry. The underlying reason is that the load distributing capability of the track grid always influences the stiffness evaluation performed by using rail deflection measurements. Consequently, other systems that are based on rail deflection measurement, like the Benkelman beam or stiffness measurement vehicles, do not allow a sleeper specific evaluation of the seat stiffness. Therefore, possible problematic sleepers (e.g. sleeper 4′ in this case study) might not be identified.

Further investigations on the correlation between stiffness variation at the individual sleeper level and vehicle reaction (e.g. axle box accelerations) are promising to enable signal evaluation methods that can be applied to track inspection.

4 CONCLUSIONS & OUTLOOK

The developed vehicle-track-subgrade coupling methodology allows the investigation of the interaction between vehicle, track and subgrade, taking into account track irregularities, vehicle dynamics, varying sleeper support and complex ballast and soil reactions, including ballast contamination.

Additionally, an iterative approach to identify individual rail seat stiffness at a measurement site was presented here. With the use of a finite element model and rail foot strain and sleeper and rail deflection measurements, rail seat stiffnesses was identified.

The presented study, focused on the effects of rail seat stiffness variation, showed that a stiffness variation, as identified in the measurement section, can lead to a changed load distribution and that individual sleepers transmitting significantly more load to the ballast than others. Ultimately, this leads to locally increased ballast deterioration and a locally increased impact on the subsoil, which might facilitate mud spot development. On the other hand, the cause of the increased sleeper load, the rail seat stiffness variation, can hardly be identified on an individual sleeper level by using loaded geometry data.

Open questions, like the causal relationships during mud spot development and other deterioration phenomena, still have to be investigated. The developed vehicle-track-subgrade coupling methodology presented here can provide a basis for future studies. Additionally, an integral coupling approach allows the detailed analysis of the vehicle reaction. Further investigations of the correlation between individual sleeper support variations and vehicle reactions may allow providing characteristic patterns for track inspection.

ACKNOWLEDGEMENTS

The authors would like to thank the German Research Foundation (DFG). The research was supported under the grants MO 2246/3-1 („Simulation punktueller Instabilitäten infolge plastischer Verformungen im Unterbau/Untergrund unter dynamischer Belastung durch Eisenbahnverkehr (EPIB 1.2)“) and FR 2910/2-1 („Detektieren von punktuellen Instabilitäten anhand typischer Rad-Schiene-Kräfte (EPIB 2)“).

REFERENCES

Chen, K., Lechner, B. and Freudenstein, S., 2018. *Investigation of track stiffness quality based on rail foot bending strain utilizing structure optimization methods*. Proceedings of 7th Transport Research Arena TRA 2018, April 16-19, 2018, Vienna, Austria.

Dahlberg, T., 2010. *Railway Track Stiffness Variations – Consequences and Countermeasures*. International Journal of Civil Engineering 8.

DB Netz AG, 2016. *Richtlinie 821 "Oberbau inspizieren"*. Munich, Germany.

Hudson, A., Watson, G., Le Pen, L. and Powrie, W., 2016. *Remediation of Mud Pumping on a Ballasted Railway Track*. Procedia Engineering, 143, 1043–1050.

Leykauf, G. and Mattner, L., 1997. *Untersuchung von Feste Fahrbahn-Konstruktionen durch eine anerkannte Prüfstelle*. Eisenbahntechnische Rundschau ETR, Edition Feste Fahrbahn (Sonderveröffentlichung), 48–55, Hestra-Verlag, Darmstadt.

Rapp, S., 2017. *Modell zur Identifizierung von punktuellen Instabilitäten am Bahnkörper in konventioneller Schotterbauweise*. Dissertation, Institute of Railway and Transportation Engineering, Faculty Civil and Environmental Engineering, University of Stuttgart, Stuttgart, Germany.

Sandner, C., Ripke, B. and Wunderlich, T., 2020. *Monitoring and evaluation of railway infrastructure*. Ingenieurvermessung 20. Beiträge zum 19. Internationalen Ingenieurvermessungskurs München, 325–338, Herbert Wichmann Verlag, Berlin, Germany.

Tennakoon, N., 2012. *Geotechnical study of engineering behaviour of fouled ballast*. Doctor of Philosophy thesis, Department of Civil, Mining and Environmental Engineering, University of Wollongong.